DOI: 10.19663/j.issn2095-9869.20220531001 http://www.yykxjz.cn/

李瑾祯, 董晨帆, 吴海燕, 邴晓菲, 冯志华, 谭志军. 栉孔扇贝对麻痹性贝类毒素的生理响应及转录组分析. 渔业科学进展, 2023, 44(6): 166–176
LI J Z, DONG C F, WU H Y, BING X F, FENG Z H, TAN Z J. Transcriptomic analysis and stress response of *Chlamys farreri* to paralytic shellfish toxins. Progress in Fishery Sciences, 2023, 44(6): 166–176

栉孔扇贝对麻痹性贝类毒素的生理响应及转录组分析

李瑾祯[1,2] 董晨帆[2] 吴海燕[2] 邴晓菲[2] 冯志华[1①] 谭志军[2,3①]

(1. 江苏省海洋生物资源与环境重点实验室 江苏海洋大学 江苏 连云港 222000；
2. 中国水产科学研究院黄海水产研究所 农业农村部水产品质量安全检测与评价重点实验室 山东 青岛 266071；
3. 青岛海洋科学与技术试点国家实验室 山东 青岛 266071)

摘要 本研究将栉孔扇贝(*Chlamys farreri*)暴露于塔玛亚历山大藻(*Alexandrium tamarense*)，通过测定内脏团中毒素的蓄积含量、氧化应激酶活性及其基因转录调控变化，探究栉孔扇贝暴露于麻痹性贝类毒素(Paralytic shellfish toxin, PSTs)的初期应激响应机制。结果显示，PSTs 在内脏团中迅速蓄积，实验第 6 天时毒素含量最高，实验第 30 天时毒素残留量高达 62.4%；PSTs 引发栉孔扇贝体内脂质过氧化，过氧化物酶(POD)、超氧化物歧化酶(SOD)及谷胱甘肽过氧化物酶(GSH-Px)显著应激($P<0.05$)。透射电镜下观察组织病变，发现空泡化、染色质聚集和核质固缩等结构损伤。通过加权基因共表达网络分析鉴定细胞凋亡和谷胱甘肽代谢解毒通路显著应激上调，映射 *ALOX5*、*AfGST-σ11*、*caspase-8* 及 *Bax* 4 个关键转录因子。综上可知，除抗氧化应激外，栉孔扇贝可激活特征性细胞凋亡和以谷胱甘肽解毒代谢反应抵抗 PSTs 毒性作用。本研究可为深入探索栉孔扇贝应激与代谢 PSTs 的特征机制提供科学依据。

关键词 麻痹性贝类毒素；栉孔扇贝；生理响应；细胞凋亡；转录组
中图分类号 S917.4 **文献标识码** A **文章编号** 2095-9869(2023)06-0166-11

麻痹性贝类毒素(Paralytic shellfish toxin, PSTs)因其分布广、毒性强等特征而被认为是目前世界上危害最大的藻神经毒素之一(Fernández-Reiriz *et al*, 2008)。研究发现，PSTs 极易在双壳贝类中大量蓄积，通过复杂的代谢转化生成 50 余种衍生物(Wiese *et al*, 2010)，并通过食物链传递，导致消费者出现恶心呕吐、肌肉麻痹、呼吸困难甚至窒息等症状，引发人类食物中毒事件(Etheridge, 2010)。因此，国际上针对 PSTs 建立了 800 μg STX eq/kg 的广泛适用的限量标准(刘智勇等, 2006)。塔玛亚历山大藻(*Alexandrium tamarense*)是中国沿海的优势产毒藻之一(Lilly *et al*, 2010)，在渤海、黄海、长江口附近沿海水域和南海部分海湾均有分布(Li *et al*, 2020a、b; 窦勇等, 2015; 过锋等, 2011)。近年来调查发现，栉孔扇贝(*Chlamys farreri*)中 PSTs 检出率、超标率均较高(钱蓓蕾等, 2012; 杜克梅等, 2013; 刘斌等, 2021)，且具有毒素蓄积速度快、代谢慢的特点(Bricelj *et al*, 1998)，其内脏团是 PST 吸收和净化过程中的主要储存库，占总毒性的

* 国家重点研发计划(2017YFC1600701)和国家自然科学基金面上项目(41806138; 31772075; 32072329)共同资助。李瑾祯，E-mail: jinzhen_li@163.com
① 通信作者：冯志华，教授，E-mail: fengzhihua@jou.edu.cn; 谭志军，研究员，E-mail: tanzj@ysfri.ac.cn
收稿日期: 2022-05-31，收修改稿日期: 2022-06-15

80%~98% (Estrada *et al*, 2007a)。

PSTs 是一种神经性毒素，其毒性作用为阻断钠离子通道并抑制神经传导。研究表明，双壳贝类暴露于 PSTs 后，主要的应激反应包括产生大量活性氧(ROS)，诱导抗氧化应激(包括酶促和非酶促防御)反应(Sebastian *et al*, 2011)、细胞内氧化还原稳态失衡(Estrada *et al*, 2007b)和导致细胞损伤(即脂质过氧化)(Qiu *et al*, 2013)。丙二醛(MDA)作为脂质过氧化的主要产物之一，其含量变化水平能直接反映 PSTs 引起的组织细胞膜损伤情况(梁忠秀等, 2014)。另外，超氧化物歧化酶(SOD)、过氧化物酶(POD)常被作为抗氧化水平评价指标，谷胱甘肽过氧化物酶(GSH-Px)是在抗氧化防御中发挥作用的关键酶(Hlaing *et al*, 2020)。现有研究常用脂质过氧化水平和抗氧化酶的改变来反映生物体的损伤与应激程度(Tsikas, 2017)。也有研究表明，PSTs 可造成组织损伤并引发栉孔扇贝基因异常表达(Lian *et al*, 2019; Hu *et al*, 2019)，但目前仍缺乏关于 PSTs 引发栉孔扇贝组织损伤的基因表达变化及调控机制的研究。

因此，本研究以一株分离自我国南海海域的产 PSTs 的塔玛亚历山大藻 AT5-3 株为实验对象，以目前我国 PSTs 残留严重的栉孔扇贝为受试动物进行暴露实验，通过在 PSTs 暴露过程中栉孔扇贝内脏团细胞的超微结构、脂质过氧化关键指标和关键抗氧化酶活性变化等指标探究栉孔扇贝的损伤与生理响应情况，通过对关键节点的转录组分析，解析在损伤和应激过程中的差异富集通路和表达基因。通过科学评价 PSTs 对栉孔扇贝损伤情况及诱发机体应激的相关机理，以期为建立与完善食品安全风险评价技术提供参考。

1　材料与方法

1.1　实验材料

本实验所用产 PSTs 毒藻为一株分离自中国南海海域的塔玛亚历山大藻 AT5-3 株，由中国科学院海洋研究所提供。该毒藻在实验室中以温度(20±1) ℃、光照 54 μ/(Em^2·s)、光暗比 12 h：12 h 的条件，使用 L1 Medium 培养液进行单种培养。选择处于指数生长期，细胞密度为 4×10^4~4.2×10^4 cells/mL 的藻液用于暴露实验。小球藻作为饵料藻同时培养，培养条件同 AT5-3 株。

本研究所用实验动物为 2 龄栉孔扇贝，产自山东省青岛市灵山湾养殖海域，正式实验前进行饥饿处理 2 d。所用海水取自青岛海域，实验期间水温控制在(16±1) ℃，保持全天不间断充气。

1.2　栉孔扇贝暴露实验

随机选取 120 只栉孔扇贝置于 6 个养殖筐，设立对照组和实验组。实验共开展 20 d，分暴露阶段(0~6 d)和代谢阶段(6~20 d)，暴露阶段 2 次/d 定时投喂指数生长期的塔玛亚历山大藻(AT5-3 株)，投喂量为 8×10^6 cells/(ind.·d)。代谢阶段投喂等量小球藻。

1.3　毒素含量测定

分别于第 0、6、14 和 20 天随机取栉孔扇贝 5 只，蒸馏水冲洗污泥及附着物后，在冰上迅速解剖分离其内脏团，均质后称量(5.00±0.05) g 样品于 50 mL 离心管中，加入 5 mL 1%乙酸水溶液，涡旋混合 90 s 后沸水浴 5 min，于流水下迅速冷却至室温，4 500 r/min 离心 10 min。取上清液 1 mL 于 2 mL 离心管中，加 5 μL 氨水涡旋混匀，10 000 r/min 离心 5 min。依次用 3 mL 乙腈，3 mL 20%乙腈水溶液(含 1%乙酸)、3 mL 0.1%氨水溶液活化 Supelco ENVI-Carb 固相萃取柱，加入提取液后用 700 μL 超纯水淋洗，再用 1 mL 75%乙腈水溶液(含 0.25%甲酸)洗脱混匀，最后 13 000 r/min 离心 10 min，取上清液于–80 ℃条件下保存待测。

采用外标法定量，用 75%乙腈水(含 0.25%甲酸)稀释 PSTs 标准品溶液配制成标准储备液，再将标准储备液稀释为基质标准工作液。用四极杆–线性阱复合型液相色谱质谱联用仪、HILLIC 色谱柱进行检测，质谱条件参考张海涛等(2021)的研究。

1.4　透射电镜样品制备与观察

分别取对照组(X-C)、实验第 6 天 (X-6)、实验第 14 天 (X-14)栉孔扇贝各 3 只，在冰上分离其内脏团，将组织切成 2 mm×2 mm×1 mm 的小块后用 2.5%戊二醛溶液固定，超薄切片制备方法参照甄静静等(2018)，使用透射电子显微镜(日立 H7000)观察切片并拍照。

1.5　生理指标测定样品

分别取对照组(C)、实验第 1 天、实验第 3 天、实验第 6 天栉孔扇贝各 3 只，在冰上分离各组织之后准确称量，随后加入任氏生理盐水，加入比例为重量(g)：体积(mL)= 1：9。冰水浴中匀浆，随后 4 ℃ 2 500 r/min 离心 10 min，取上清液转移至新的 1.5 mL 离心管中，于液氮中保存。按 MDA、POD、GSH-Px 和 SOD 试剂盒(南京建成科技有限公司)说明书分别测定其含量及活力。

1.6　转录组分析

分别取对照组(X-C)、实验第 3 天 (X-3)、实验第

6 天 (X-6)栉孔扇贝各 3 只，冰上取其内脏团后使用液氮迅速冷冻。由北京百迈客生物科技有限公司进行 RNA 提取、cDNA 文库构建及高通量测序。使用 TRIzol 试剂提取内脏团总 RNA，浓度用 NanoDrop 2000 (ThermoFisher Scientific，美国)检测，完整性用 Agilent 2100 (Agilent Technologies，美国)检测。检测合格后进行 cDNA 文库构建，并使用 Illumina HiSeq (Illumina 公司，美国)进行测序。

将得到原始序列进行过滤后得到高质量 clean reads，并使用 Trinity 软件进行 de novo 组装。取每条基因中最长的转录本作为 unigenes 与 KEGG 数据库进行序列比对得到注释信息。

以 FPKM 值衡量基因表达水平，以校正后的 *P* 值(Fold change)<0.05 且错误发现率(FDR)≥2 作为标准筛选差异表达基因(DEGs)，随后用 DSEeq2 软件对 DEGs 进行分析。最后在 KEGG、GO 数据库中对 DEGs 进行注释和功能富集分析(以 *P*<0.05 为富集标准)以探究 DEGs 功能及其与代谢物之间的关系。

1.7 基因共表达网络构建

在 R 软件中运行 R 包，剔除离群值后构建 WGCNA 基因共表达网络，选择适当 β 值，构建拓扑重叠矩阵，再绘制基因的层次聚类树，以皮尔逊相关系数(*r*)为指标选择目标模块进行 KEGG 注释，随后使用 cytoscape 软件绘制基因互作网络分析图，以寻找核心调控基因。

2 结果

2.1 栉孔扇贝毒素蓄积与超微结构损伤

PSTs 在内脏团中的蓄积含量呈现先升后降的趋势，在实验第 6 天时达到峰值，最高蓄积含量超出限量标准 15 倍左右(图 1a)。蓄积速率由快转慢，结束毒素暴露后，PSTs 在栉孔扇贝内脏团中缓慢代谢，代谢 14 d 后 PSTs 含量仍然超出限量标准，残留率高达 62.4%。透射电镜观察发现内脏团随 PSTs 暴露时间出现明显组织结构损伤，主要包括肠上皮细胞间黏附力下降、部分细胞的细胞膜及线粒体等细胞器消

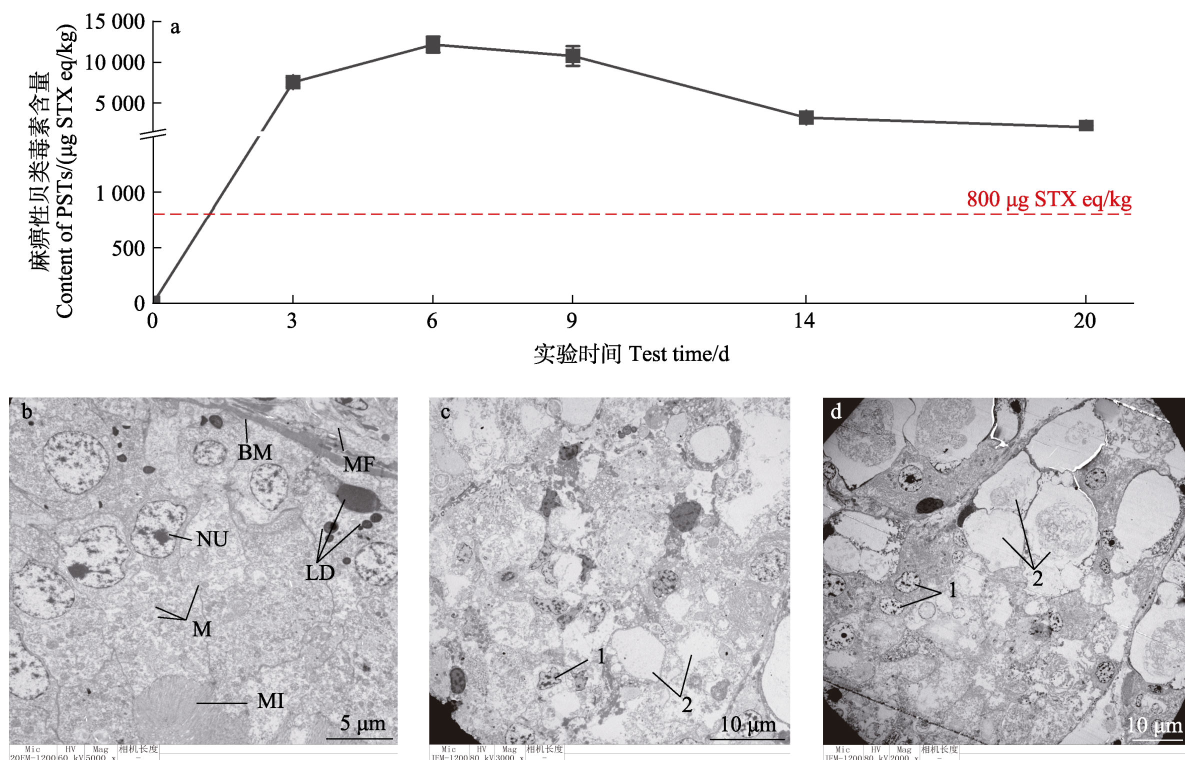

图 1 不同时间栉孔扇贝中 PSTs 蓄积量和内脏团组织超微结构变化

Fig.1 The accumulation of PSTs and its ultrastructural damage in *C. farreri*

a：PSTs 在内脏中的蓄积含量；b：对照组；c：X-6 组；d：X-14 组。NU：细胞核；M：线粒体；MI：微绒；BM：基底膜；MF：肌纤维；LD：脂滴。1：细胞核质固缩、染色质凝聚；2：细胞空泡化，细胞膜、线粒体等细胞器消失。

a: Accumulation of PSTs in viscera; b: Normal scallops; c: *C. farreri* exposed for 6 days; d: *C. farreri* exposed for 14 days; NU: Nucleus; M: Mitochondria; MI: Microvilli; BM: Basement membrane; MF: Muscle fiber; LD: Lipid droplets. 1: Cytoplasmic pyknosis, chromatin condensation; 2: Cell vacuoles and the cell membrane, mitochondria and other organelles disappeared.

失，并出现了细胞核质固缩、染色质凝聚和细胞空泡化现象(图 1c)，实验第 14 天时虽然毒素含量下降，但组织损伤更为严重(图 1d)。

2.2　栉孔扇贝对 PSTs 的抗氧化反应

测定 MDA、GSH-Px、POD 和 SOD 四项指标用以评估栉孔扇贝的抗氧化应激水平。结果如图 2 所示，内脏团中 MDA、GSH-Px 和 POD 的应激活跃，SOD 则被显著抑制($P<0.05$)。毒素暴露期 MDA 的含量升高较为显著($P<0.05$)，在实验第 6 天时含量已达到对照组 1.38 倍。GSH-Px 的活力在暴露初期(实验第 1 天)被显著抑制，随后迅速应激，在实验第 3 天时达到峰值，但随实验时间的延长其活力再次被抑制。POD 活力显著应激，酶活力先上升后下降，活力峰值出现在实验第 3 天。SOD 则呈现与 POD 相反的活力变化趋势，实验第 3 天时活力最低，实验第 6 天时活力有所回升，但仍低于正常水平。

2.3　转录组分析

通过 RNA-seq，本研究分别构建了栉孔扇贝对照组(X-C-1、X-C-2、X-C-3)、实验第 3 天(X-3-1、X-3-2、X3-3)和实验第 6 天(X-6-1、X-6-2、X-6-3)内脏团的 cDNA 文库，过滤后获得高质量 clean data，Q30 均达到了 89%以上。用 Trinity 软件进行拼接组装，共得到包含 441 749 条 Unigenes 和 624 887 个 Transcripts，平均长度为 562 bp，N50 为 802 bp。

KEGG 富集分析共筛选到 933 个 DEGs 以表达上调为主，其中，X-3 组表达上调最多，而 X-6 组表达下调居多(图 3)。主要注释在代谢相关通路(占比 50%)，包括氨基酸代谢及碳水化合物代谢。对照组与实验第 3 天比较，DEGs 主要富集在丙酮酸代谢、糖酵解/糖异生、脂肪酸代谢等通路，实验第 3 天与第 6 天相比，DEGs 主要富集在丙酮酸代谢、磷酸戊糖途径、糖酵解/糖异生等通路。

2.4　WGCNA 分析

对所有 DEGs 进行 WGCNA 分析。结果表明，DEGs 被聚类为若干模块(图 4a)，其中包括蓝紫色和浅橙色在内的 8 个模块基因与 PSTs 蓄积呈显著正相关($r \geqslant 0.9$)，对其基因进行 KEGG 富集分析(图 4b)，结果显示，基因显著富集于细胞吞噬与凋亡(溶酶体、吞噬体、细胞凋亡与胞吞作用)及代谢相关途径(花生四烯酸代谢、ABC 转运、细胞色素 P450 对外源化合物的代谢与谷胱甘肽代谢)。对正相关模块基因进行

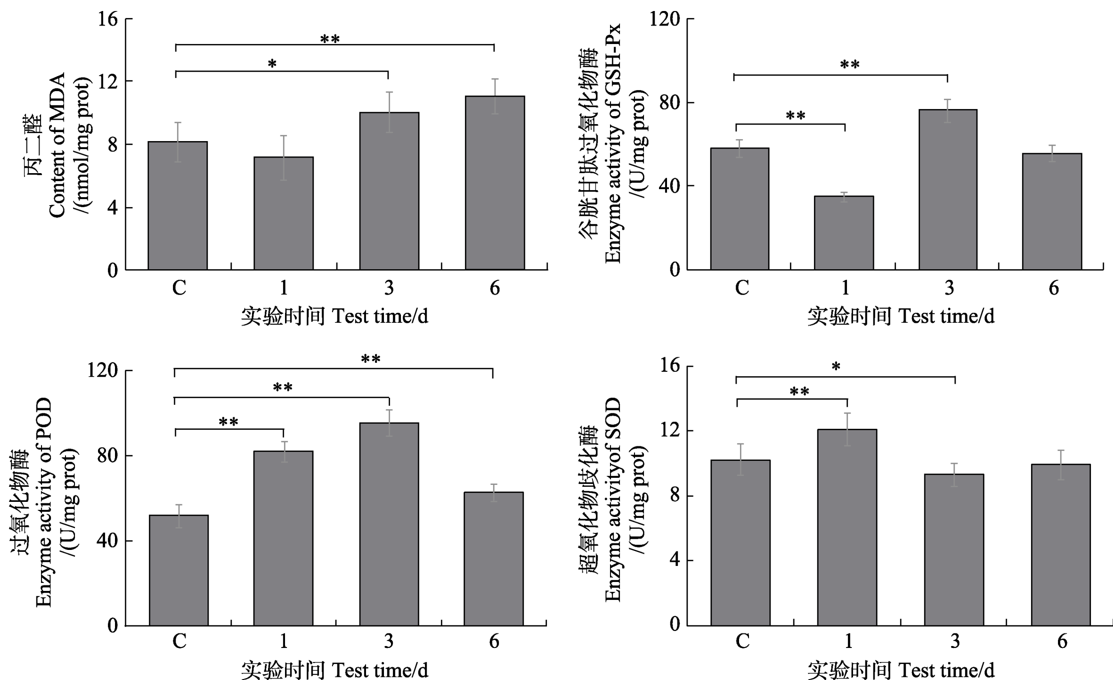

图 2　栉孔扇贝内脏团中 MDA 含量及 GSH-Px、POD、SOD 酶活力变化

Fig.2　Changes of MDA content and GSH-Px, POD, SOD enzyme activities in visceral mass of *C. farreri*

C 为对照组，“*”表示与对照组相比差异显著($P<0.05$)，“**”表示与对照组相比差异极显著($P<0.01$)，下同。

C is the control group, “*” means significant difference compared with the control group ($P<0.05$), “**” means extremely significant difference compared with the control group ($P<0.01$), the same below.

MDA: Malondialdehyde; GSH-Px: Glutathione peroxidase; POD: Peroxidase; SOD: Superoxide dismutase.

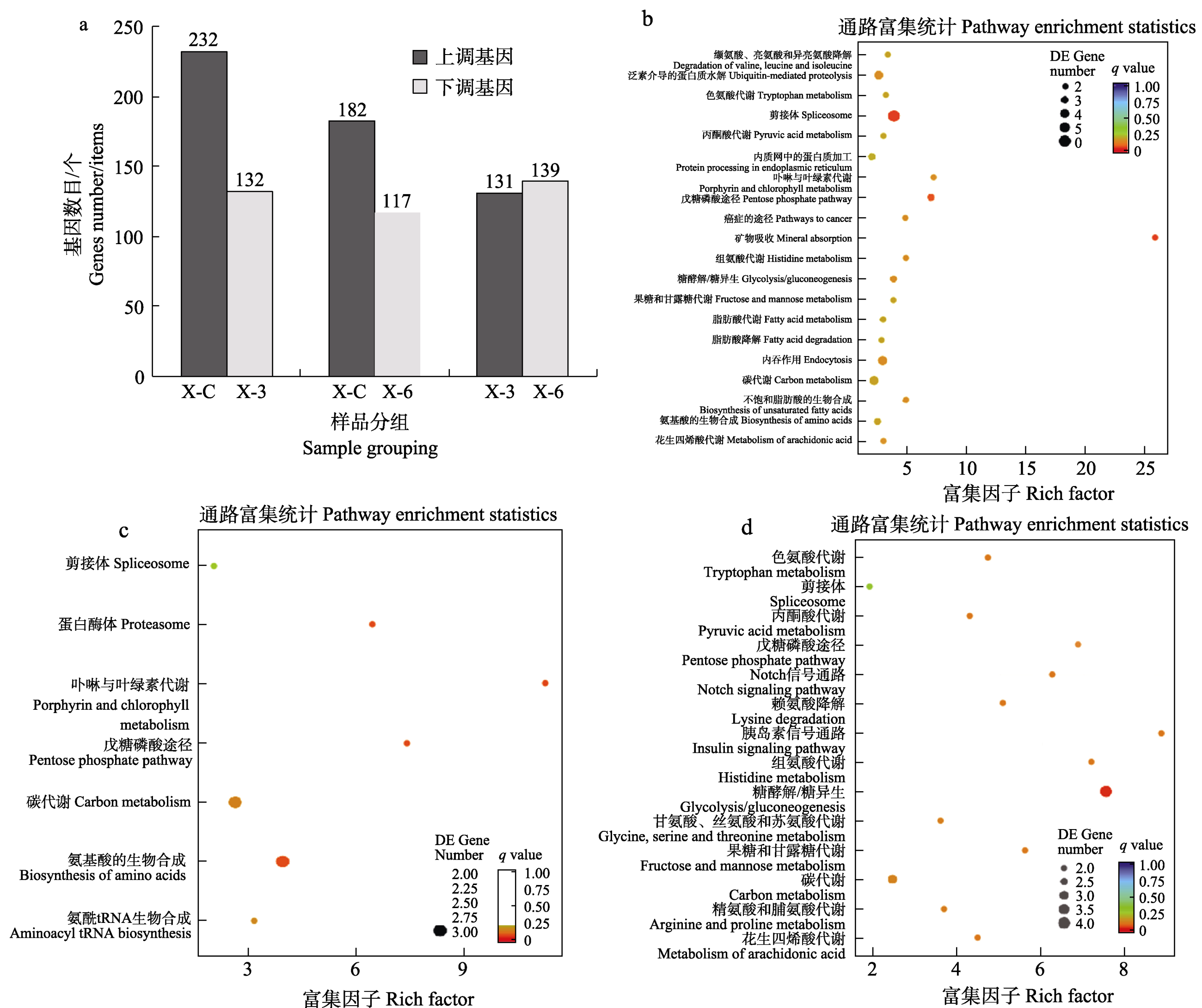

图 3 栉孔扇贝内脏团差异表达基因数目及 KEGG 注释结果(Top 20)

Fig.3 Number of differentially expressed genes in visceral mass of *C. farreri* and KEGG annotation

a：差异基因数目；b：X-C 与 X-3 的 DEGs 显著富集结果(KEGG)；c：X-C 与 X-6 的 DEGs 显著富集结果(KEGG)；d：X-3 与 X-6 的 DEGs 显著富集结果(KEGG)。各组别只展示富集最为显著的前 20 条，不足 20 条的全部展示。

a: Number of differential genes; b: Significant enrichment results of DEGs of X-C and X-6 (KEGG); c: Significant enrichment result of DEGs of X-C and X-6 (KEGG); d: Significant enrichment result of DEGs of X-3 and X-6 (KEGG). Each group only showed the first 20 items with the most significant enrichment, and less than 20 items were displayed in full.

相互作用分析，发现有 242 个模块基因相互作用，协同应激 PSTs 暴露，其中 4 个高通量差异基因在应激过程中发挥关键调控作用(图 4c)。

上述 4 个发挥关键调控作用的基因中被注释为 *ALOX5*、*AfGST3-1*、*caspase-8* 及 *Bax4*。分别将其在不同时间点的 FPKM 值为纵坐标作图(图 5)。结果表明，与对照组相比，4 种基因的表达量均存在显著差异($P<0.05$)，其中，*ALOX5*、*AfGST3-1* 有相似的表达模式，表达量随实验时间的延长呈先升后降趋势，在实验第 3 天表达量最高，实验第 6 天时表达量有所降低，但仍为极显著过表达($P<0.01$)。*caspase-8* 和 *Bax* 表达模式相似，表达量随实验时间的延长而逐渐升高，实验第 6 天表达量最高，均为极显著过表达($P<0.01$)。

3 讨论

现有研究表明，栉孔扇贝暴露 PSTs 的主要应激包括抗氧化、组织损伤和代谢解毒等反应。上述抗氧化反应可显著降低由于 PSTs 暴露造成的过氧化损伤(Oyaneder-Terrazas *et al*, 2022)。本研究观察到栉孔扇

贝机体存在短暂的氧化应激反应以消除脂质过氧化，表现为抗氧化酶 SOD、POD 分别在实验第 1、3 天时显著应激(*P*<0.05)。但在毒素含量最高时抗氧化酶酶活被抑制，组织严重损伤。与本研究相似，Oyaneder-Terrazas 等(2022)研究表明，贻贝(*Mytilus chilensis*)、蛤蜊(*Ameghinomya antiqua*)等在贝类体内抗氧化酶活性 PSTs 暴露初期显著升高，暴露末期显著降低且氧化损伤加重。这主要是因为扇贝对 PSTs 的蓄积具有耐受性强、代谢慢的特点(Oshima *et al*, 1982; Escobedo-Lozano *et al*, 2012)，栉孔扇贝体内高残留的 PSTs 诱发的持续性脂质过氧化损伤(Choi *et al*, 2006)，进而成为细胞持续凋亡的诱因之一。

近年来，由 PSTs 暴露诱发的细胞凋亡现象在牡蛎(Medhioub *et al*, 2013)、蛤蜊、贻贝(Sokolova *et al*, 2004a; Mat *et al*, 2013a; Rolland *et al*, 2014)等均已报道。本研究中观察到了 PSTs 对栉孔扇贝内脏团组织造成的损伤，主要表现为线粒体等细胞器消失、细胞核萎缩等，同时观察到染色质凝聚和膜消失(膜损伤)。其中，染色质凝聚及膜损伤被认为是细胞凋亡的标志(Snigirevskaya *et al*, 2019)。此外，本研究观测到 PSTs 可显著升高 MDA 含量(*P*<0.05)，在毒素含量蓄积最高时，MDA 含量极显著升高(*P*<0.01)，说明 PSTs 会在栉孔扇贝内脏团中诱发脂质过氧化反应，且脂质过氧化程度可能与 PSTs 含量正相关。MDA 的含量变化是机体脂质过氧化水平的重要表征。赤潮藻所产毒素对贝类造成的脂质过氧化损伤则是触发细胞凋亡的重要原因之一(Ricevuto *et al*, 2016; De *et al*, 2017)。最后通过比较 WGCNA 及 KEGG 注释结果均表明细胞

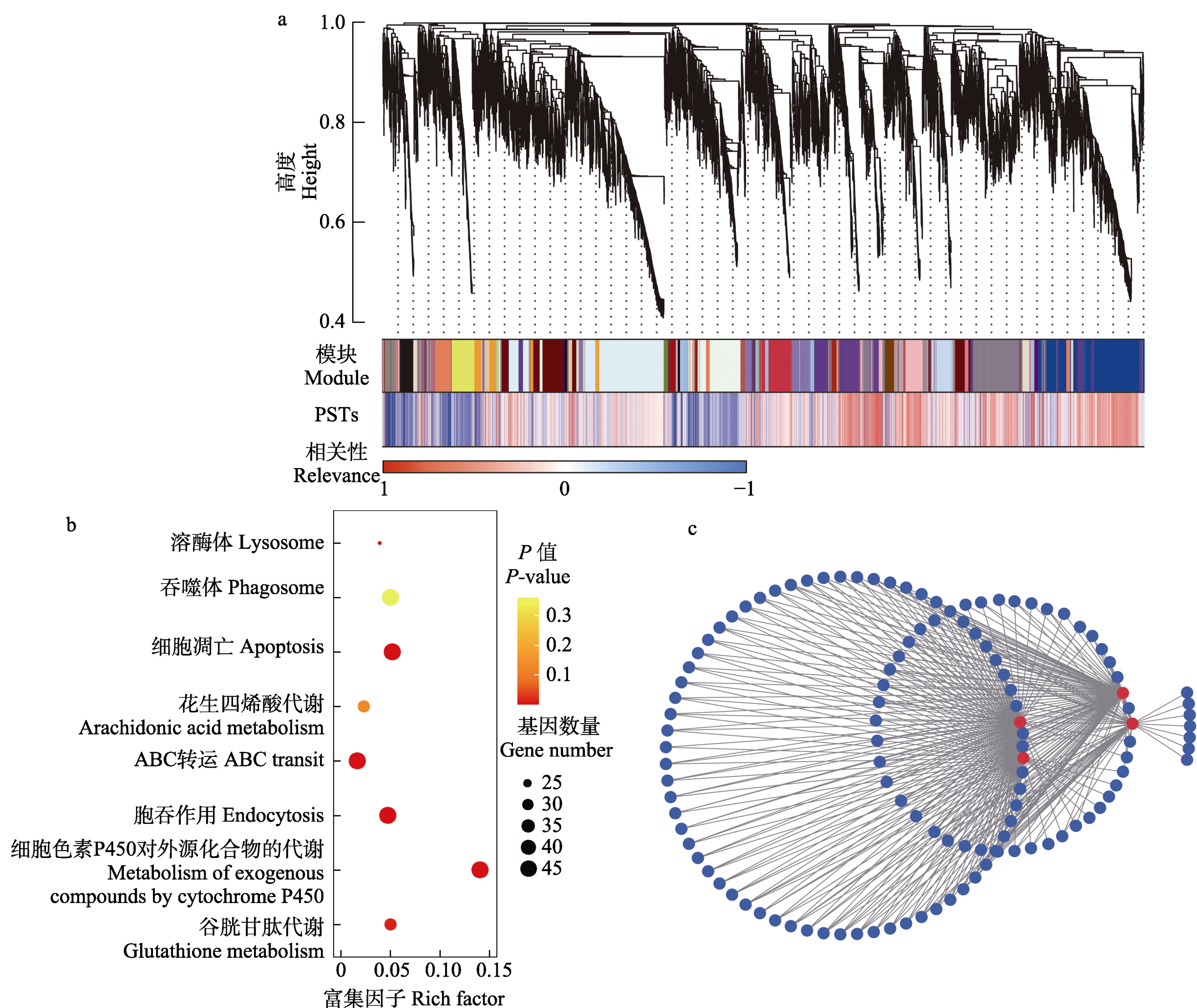

图 4　差异基因富集与 WGCNA 分析结果

Fig.4　Differential gene enrichment and WGCNA analysis result

a：WGCNA 分析差异基因与 PSTs 蓄积相关性；b：正相关模块基因富集分析；c：正相关模块基因相互作用分析。

a: WGCNA analysis of PSTs exposure correlation; b: Gene enrichment analysis of positive correlation module; c: Gene interaction analysis of positive correlation module.

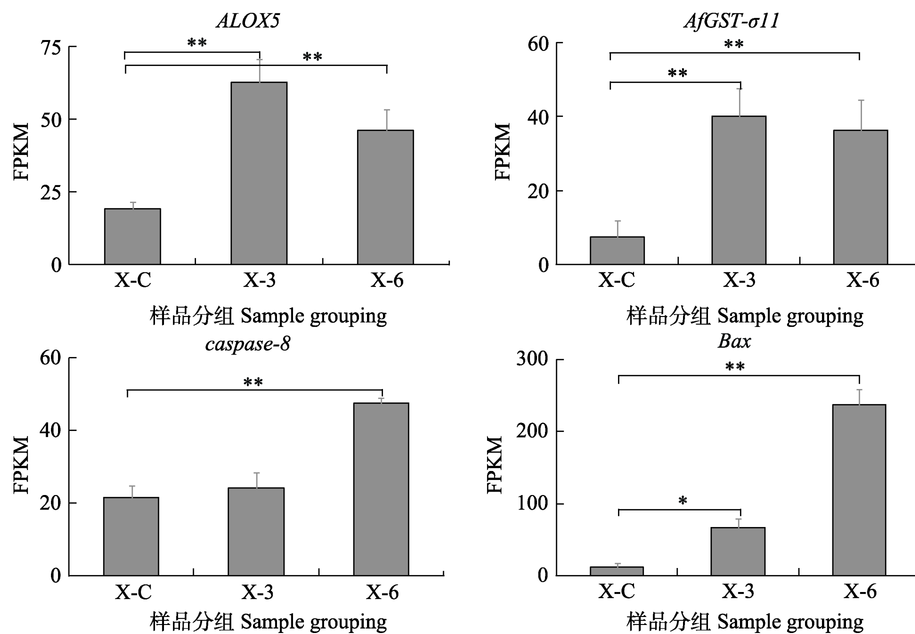

图 5 关键调控基因在不同时期的表达变化
Fig.5 Expression changes of key regulatory genes in different periods

凋亡与 PSTs 的蓄积含量呈显著正相关。综上所述，PSTs 暴露造成的机体损伤诱发栉孔扇贝细胞凋亡。

半胱氨酸天冬氨酸蛋白酶(*caspase*)基因家族是引发细胞凋亡的主要执行者，Abi-Khalil 等(2017)已证明 PSTs 可通过 *caspase* 基因家族介导的途径诱发牡蛎血细胞发生凋亡。本研究中，*caspase* 基因家族在不同实验时间也存在差异表达，包括凋亡启动相关基因 *caspse-2/9* 和 *caspase-8/10* 以及凋亡执行基因 *caspase-3/7*，其中 *caspase-8* 表达尤为显著，在不同实验时间的表达量存在显著差异(P<0.01)。*caspase-8* 在细胞凋亡过程中承担分子开关的作用(Calderón-Garcidueñas *et al*, 2008)，有研究表明，将 GTX2/3 暴露扇贝后，*caspase-8* 的活性增加(Estrada *et al*, 2014)。且基因 *caspase-8* 仅在成年扇贝的消化腺和肾脏中高表达(Wei *et al*, 2022)。由此进一步推断，凋亡启动基因 *caspase-8* 过量表达触发的凋亡机制或是成年栉孔扇贝应激 PSTs 暴露的特征反应机制。与此同时，基因 *Bax* 在控制细胞凋亡的过程中发挥重要作用，可通过增强线粒体膜的通透性，促进促凋亡蛋白的释放(Bock *et al*, 2019)。Medhioub 等(2013)研究发现，暴露于 PSTs 的牡蛎血细胞中基因 *Bax* 显著过表达(P<0.01)。在本研究中，PSTs 造成了栉孔扇贝内脏团组织细胞中基因 *Bax* 显著过表达(P<0.05)，且受含量影响在毒素蓄积量最高时(X-6 组)表达量极显著升高(P<0.01)。表明基因 *Bax* 可能参与 PSTs 引发栉孔扇贝内脏团细胞凋亡的调控机制。

栉孔扇贝可激活解毒代谢机制以减轻毒素损伤。贝类的解毒代谢机制主要分为 3 个阶段。第一阶段对异生物质进行酶修饰，可直接或间接中和 PST 并将其转化为 ROS，细胞色素 P450 在这一阶段发挥重要作用(Rolland *et al*, 2014)；第二阶段为带电物质与包括谷胱甘肽在内的极性化合物的结合(Fabioux *et al*, 2015)；第三阶段依赖于膜转运蛋白介导的毒素外排，包括多药耐药蛋白(MRP)和 ATP 结合转运蛋白盒家族成员(ABC)(Wang *et al*, 2021)。Freitas 等(2020)研究表明，暴露于 PSTs 的贻贝、鸟蛤(Galbuliformes)、竹蛏(*Solen strictus*)中谷胱甘肽代谢通路被激活。本研究的酶活结果显示，PSTs 暴露后 GSH-Px 活力显著升高(P<0.05)，转录组结果表明，谷胱甘肽代谢通路被显著富集。此外，WGCNA 结果显示，细胞色素 P450 对外源化合物的代谢、谷胱甘肽代谢及 ABC 转运通路均与 PSTs 暴露显著正相关，表明 PSTs 的暴露已激起栉孔扇贝体内谷胱甘肽的解毒应激。说明 PSTs 激活了栉孔扇贝毒素代谢机制。Hlaing 等(2020)研究表明，PSTs 可引起栉孔扇贝中 *CfGST3* 相关基因的特异性表达，该亚家族在抵御毒素损伤时可发挥多项功能。但本研究表明，持续高浓度的毒素暴露仍将造成组织损伤，由此可知，栉孔扇贝机体的抗氧化及解毒代谢能力有限，无法保护栉孔扇贝机体免受脂质过氧化损伤。

4　结论与展望

PSTs 在栉孔扇贝体内具有高蓄积，高残留的特征，诱发栉孔扇贝机体持续的抗氧化应激与组织损伤。细胞凋亡可能是栉孔扇贝应激 PSTs 暴露的防御手段之一。栉孔扇贝暴露于 PSTs 产毒藻 AT5-3 后，机体受到脂质过氧化损伤后诱发由 *caspase-8* 特征性启动的细胞凋亡程序，促进了栉孔扇贝机体对 PSTs 的内源性代谢，以维护自身内环境平衡。为保护自身，栉孔扇贝机体抗氧化酶系统及解毒代谢机制快速应激，但效果有限，无法消除高残留 PSTs 诱发的持续性损伤。这为以后更加深入地研究 PSTs 对栉孔扇贝的潜在毒性以及栉孔扇贝的免疫分子机制提供了基础。

参　考　文　献

ABI-KHALIL C, FINKELSTEIN D S, CONEJERO G, *et al*. The paralytic shellfish toxin, saxitoxin, enters the cytoplasm and induces apoptosis of oyster immune cells through a caspase-dependent pathway. Aquatic Toxicology, 2017, 190(1): 133–141

BOCK F J, TAIT SWG. Mitochondria as multifaceted regulators of cell death. Nature Reviews Molecular Cell Biology, 2020, 21(2): 85–100

BRICELJ V M, SHUMWAY S E. Paralytic shellfish toxins in bivalve molluscs: Occurrence, transfer kinetics, and biotransformation. Reviews in Fisheries Science, 1998, 6(4): 315–383

CALDERON-GARCIDUENAS L, SOLT A C, CARLOS H R, *et al*. Apoptosis: A review of programmed cell death. Toxicologic Pathology, 2008, 36(2): 289–310

CHOI N M , YEUNG L W, SIU W H, *et al*. Relationships between tissue concentrations of paralytic shellfish toxins and antioxidative responses of clams, *Ruditapes philippinarum*. Marine Pollution Bulletin, 2006, 52(5): 572–578

DOU Y, GAO J W, SHI X T, *et al*. Outbreak frequency and factors influencing red tides in nearshore waters of the South China Sea from 2000 to 2013. Journal of Hydroecology, 2015, 36(3): 31–37 [窦勇, 高金伟, 时晓婷, 等. 2000—2013 年中国南部近海赤潮发生规律及影响因素研究. 水生态学杂志, 2015, 36(3): 31–37]

DU K M, LEI F, WU N, *et al*. The pattern of paralytic shellfish poisoning in shellfish cultured in East China Sea and South China Sea. Journal of Jinan University (Natural Science & Medicine Edition), 2013, 34(3): 343–346 [杜克梅, 雷芳, 吴霓, 等. 我国东海和南海近岸海域麻痹性贝类毒素污染状况. 暨南大学学报(自然科学与医学版), 2013, 34(3): 343–346]

ESCOBEDO-LOZANO A Y, ESTRADA N, ASCENCIO F, *et al*. Accumulation, biotransformation, histopathology and paralysis in the Pacific Calico Scallop *Argopecten ventricosus* by the paralyzing toxins of the dinoflagellate *Gymnodinium catenatum*. Marine Drugs, 2012, 10(4): 1044–1065

ESTRADA N A, LAGOS N, GARCÍA C, *et al*. Effects of the toxic dinoflagellate *Gymnodinium catenatum* on uptake and fate of paralytic shellfish poisons in the Pacific giant lions-paw scallop *Nodipecten subnodosus*. Marine Biology, 2007a, 151(4): 1205–1214

ESTRADA N, ASCENCIO F, SHOSHANI L, *et al*. Apoptosis of hemocytes from lions-paw scallop *Nodipecten subnodosus* induced with paralyzing shellfish poison from *Gymnodinium catenatum*. Immunobiology, 2014, 219(12): 964–974

ESTRADA N, DE JESÚS REMERO M, CAMPA-CÓRDOVA A, *et al*. Effects of the toxic dinoflagellate, *Gymnodinium catenatum* on hydrolytic and antioxidant enzymes, in tissues of the giant lions-paw scallop *Nodipecten subnodosus*. Comparative Biochemistry and Physiology, Part C, 2007b, 146(4): 502–510

ETHERIDGE S M. Paralytic shellfish poisoning: Seafood safety and human health perspectives. Toxicon, 2010, 56(2): 108–122

FABIOUX C, SULISTIYANI Y, HABERKORN H, *et al*. Exposure to toxic *Alexandrium minutum* activates the detoxifying and antioxidant systems in gills of the oyster *Crassostrea gigas*. Harmful Algae, 2015, 48(9): 55–62

FERNÁNDEZ-REIRIZ M J, NAVARRO J M, CONTRERAS A M, *et al*. Trophic interactions between the toxic dinoflagellate *Alexandrium catenella* and *Mytilus chilensis*: Feeding and digestive behaviour to long-term exposure. Aquatic Toxicology, 2008, 87(4): 245–251

FREITAS J S, TERESA F B, DE ALMEDIA E A, *et al*. Influence of temperature on the antioxidant responses and lipid peroxidation of two species of tadpoles (*Rhinella schneideri* and *Physalaemus nattereri*) exposed to the herbicide sulfentrazone (Boral 500SC$^{(R)}$). Comparative Biochemistry and Physiology Toxicology and Pharmacology: CBP, 2017, 197: 32–44

FREITAS R, MARQUES F, MARCHI L D, *et al*. Biochemical performance of mussels, cockles and razor shells contaminated by paralytic shellfish toxins. Environmental Research, 2020, 188: 109846

GUO F, CUI Y, CHEN B J, *et al*. Analysis of toxic and harmful substances in shellfish of Jiaozhou Bay. Progress in Fishery Sciences, 2011, 32(6): 115–120 [过锋, 崔毅, 陈碧鹃, 等. 胶州湾贝类体内有毒有害物质污染状况分析. 渔业科学进展, 2011, 32(6): 115–120]

HLAING S M M, LOU J, CHENG J, *et al*. Tissue-biased and species-specific regulation of glutathione peroxidase (GPx) genes in scallops exposed to toxic dinoflagellates. Toxins (Basel), 2020, 13(1): 21

HU B, LI M, YU X, *et al*. Diverse expression regulation of Hsp70 genes in scallops after exposure to toxic *Alexandrium*

dinoflagellates. Chemosphere, 2019, 234: 62–69

LI D, GENG H X, YU R C, *et al*. Distribution of *Alexandrium pacificum* cysts in the area adjacent to the Changjiang River estuary, China. Marine Pollution Bulletin, 2020b, 156: 111206

LI D, YU R C, GENG H X, *et al*. Resting cysts of *Alexandrium catenella* and *A. pacificum* (Dinophyceae) in the Bohai and Yellow Seas, China: Abundance, distribution and implications for toxic algal blooms-ScienceDirect. Harmful Algae, 2020a, 93(2): 101794

LIAN S S, ZHAO L, XUN X G, *et al*. Genome-wide identification and characterization of SODs in Zhikong scallop reveals gene expansion and regulation divergence after toxic dinoflagellate exposure. Marine Drugs, 2019, 17(12): 700

LIANG Z X, LI J, REN H, *et al*. Toxic dinoflagellate *Alexandrium tamarense* induces oxidative stress and up-regulae *Caspase* gene (*FcCasp*) expression in gills of Chinese shrimp, *Fenneropenaeus chinensis*. Journal of Fishery Sciences of China, 2014, 21(1): 8 [梁忠秀, 李健, 任海, 等. 塔玛亚历山大藻对中国明对虾鳃组织的氧化胁迫和对 *Caspase* 基因(*FcCasp*)表达的影响. 中国水产科学, 2014, 21(1): 8]

LILLY E L, HALANYCH K M, ANDERSON D M. Species boundaries and global biogeography of the *Alexandrium tamarense* complex (Dinophyceae). Journal of Phycology, 2010, 43(6): 1329–1338

LIU B, ZHAO H Q, LIU B, *et al*. Investigation and analysis of paralytic shellfish poison pollution in retail shellfish in Hebei province from 2018 to 2020. Journal of Food Safety and Quality, 2021, 12(5): 7 [刘斌, 赵慧琴, 刘波, 等. 2018—2020 年河北省市售贝类中麻痹性贝类毒素污染状况调查分析. 食品安全质量检测学报, 2021, 12(5): 7]

LIU Z Y, JI R. Comparison of criteria for paralytic shellfish poisons in shellfish aquatic products in various countries. China Tropical Medicine, 2006, 6(1): 3 [刘智勇, 计融. 各国贝类水产品中麻痹性贝类毒素限量标准的比对. 中国热带医学, 2006, 6(1): 3]

MAT A M, HABERKORN H, BOURDINEAUD J P, *et al*. Genetic and genotoxic impacts in the oyster *Crassostrea gigas* exposed to the harmful alga *Alexandrium minutum*. Aquatic Toxicology, 2013, 140/141: 458–465

MEDHIOUB W, RAMONDENC S, VANHOVE A S, *et al*. Exposure to the neurotoxic dinoflagellate, *Alexandrium catenella*, induces apoptosis of the hemocytes of the oyster, *Crassostrea gigas*. Marine Drugs, 2013, 11(12): 4799–4814

OSHIMA Y, YASUMOTOR T, KODAMA M, *et al*. Features of paralytic shellfish poison occurring in Tohoku District. Nsugaf, 1982, 48(4): 525–530

OYANEDER-TERRAZAS J, FIGUEROA D, ARANEDA O F, *et al*. Saxitoxin group toxins accumulation induces antioxidant responses in tissues of *Mytilus chilensis*, *Ameghinomya antiqua*, and *Concholepas concholepas* during a bloom of *Alexandrium pacificum*. Antioxidants (Basel), 2022, 11(2): 392

QIAN B L, XU J, WANG Y, *et al*. Investigation and evaluation of paralytic shellfish poison in shellfish collected from aquatic product wholesale market in Shanghai. Journal of Food Safety and Quality, 2012(2): 89–92 [钱蓓蕾, 徐捷, 王媛, 等. 上海市售贝类产品中麻痹性贝类毒素污染状况调查及其评价. 食品安全质量检测学报, 2012(2): 89–92]

QIU J B, MA F F, FAN H, *et al*. Effects of feeding *Alexandrium tamarense*, a paralytic shellfish toxin producer, on antioxidant enzymes in scallops (*Patinopecten yessoensis*) and mussels (*Mytilus galloprovincialis*). Aquaculture, 2013, 396

RICEVUTO E, LANZONI I, FATTORINI D, *et al*. Arsenic speciation and susceptibility to oxidative stress in the fanworm *Sabella spallanzanii* (Gmelin) (*Annelida, Sabellidae*) under naturally acidified conditions: An in situ transplant experiment in a Mediterranean CO_2 vent system. Science of the Total Environment, 2016, 544: 765–773

ROLLAND J L, MEDHIOU B, VERGNES A, *et al*. A Feedback mechanism to control apoptosis occurs in the digestive gland of the oyster *Crassostrea gigas* exposed to the paralytic shellfish toxins producer *Alexandrium catenella*. Marine Drugs, 2014, 12(9): 5035–5054

SEBASTIAN S E, BRENA B M, LUQUET C M, *et al*. Microcystin accumulation and antioxidant responses in the freshwater clam *Diplodon chilensis patagonicus* upon subchronic exposure to toxic Microcystis aeruginosa. Ecotoxicology and Environmental Safety, 2011, 74(5): 1188–1194

SNIGIREVSKAYA E S, KOMISSARCHIKY Y. Ultrastructural traits of apoptosis. Cell Biology International, 2019, 43(7): 728–738

SOKOLOVA I M, EVANS S, HUGHES F M. Cadmium-induced apoptosis in oyster hemocytes involves disturbance of cellular energy balance but no mitochondrial permeability transition. Journal of Experimental Biology, 2004a, 207(19): 3369–3380

SOKOLOVA I M. Apoptosis in molluscan immune defense. Invertebrate Survival Journal, 2009b, 6(1): 49–58

TSIKAS D. Assessment of lipid peroxidation by measuring malondialdehyde (MDA) and relatives in biological samples: Analytical and biological challenges. Analytical Biochemistry, 2017, 524: 13–30

WANG H, LIU S, XUN X, *et al*. Toxin- and species-dependent regulation of ATP-binding cassette (ABC) transporters in scallops after exposure to paralytic shellfish toxin-producing dinoflagellates. Aquatic Toxicology, 2021, 230: 105697

WEI Z C, DING W, LI M, *et al*. The caspase homologues in scallop *Chlamys farreri* and their expression responses to toxic dinoflagellates exposure. Toxins (Basel), 2022, 14(2):

108

WIESE M, D'AGOSTINO P M, MIHALI T K, *et al*. Neurotoxic alkaloids: Saxitoxin and its analogs. Marine Drugs, 2010, 8(7): 2185–2211

ZHANG H T, WU H Y, ZHENG G C, *et al*. Accumulation and transformation of paralytic shellfish toxin in mussel *Mytilus galloprovincialis* exposed to *Alexandrium catenella*. Progress in Fishery Sciences, 2023, 44(1): 181–190 [张海涛, 吴海燕, 郑关超, 等. 链状亚历山大藻暴露下紫贻贝体内麻痹性贝毒蓄积转化规律. 渔业科学进展, 2023, 44(1): 181–190]

ZHEN J J, YE F Y, WANG D, *et al*. Effect of cadmium on ultrastructure of gill epithelial cells in clam *Meretrix meretrix*. Fisheries Science, 2018, 37(4): 469–474 [甄静静, 叶方源, 王都, 等. 镉离子对文蛤鳃上皮细胞超微结构的影响. 水产科学, 2018, 37(4): 469–474]

(编辑　陈　辉)

Transcriptomic Analysis and Stress Response of *Chlamys farreri* to Paralytic Shellfish Toxins

LI Jinzhen[1,2], DONG Chenfan[2], WU Haiyan[2], BING Xiaofei[2], FENG Zhihua[1①], TAN Zhijun[2,3①]

(1. *Provincial Key Laboratory of Marine Biological Resources and Environment, Jiangsu Ocean University, Lianyungang* 222000, *China*; 2. *Yellow Sea Fisheries Research Institute, Chinese Academy of Fishery Sciences, National Key Laboratory of Testing and Evaluation for Aquatic Product Safety and Quality, Ministry of Agriculture and Rural Affairs, Qingdao* 266071, *China*; 3. *Pilot National Laboratory for Marine Science and Technology* (*Qingdao*), *Qingdao* 266071, *China*)

Abstract　Paralytic shellfish toxins (PSTs) are some of the most harmful algal neurotoxins in the world. They easily accumulate in bivalve shellfish and are transmitted through the food chain, causing symptoms such as nausea and vomiting, muscle paralysis, dyspnea and even asphyxiation in consumers, leading to food poisoning in humans. Therefore, a widely accepted limit standard of 800 μg STXeq/kg has been established as a safe limit for PSTs. PSTs are produced by some microalgae, among which *Alexandrium tamarense* is one of the predominant toxic algae found along the coast of China. It was found that the detection rate and over-standard rate of *Chlamys farreri* in bivalve shellfish sold in China are relatively high. PSTs are mainly stored in visceral masses and are characterized by their fast accumulation and slow metabolism.

PSTs are neurotoxins that exert their toxic effects by blocking sodium channels and inhibiting nerve conduction. Studies have shown that PSTs can cause stress responses in bivalves, including production of a large amount of reactive oxygen species (ROS), antioxidant stress (including enzymatic and non-enzymatic defense), imbalance of intracellular redox homeostasis, and cell damage (i.e., lipid peroxidation). As one of the main products of lipid peroxidation, the content of malondialdehyde (MDA) can directly reflect tissue and cell membrane damage caused by PSTs. In addition, superoxide dismutase (SOD) and peroxidase (POD) are often used as indicators to evaluate the level of antioxidation, and glutathione peroxidase (GSH-Px) plays a key role in antioxidant defense. The changes in lipid peroxidation and antioxidant enzymes are commonly used in existing studies to reflect the injury and degree of stress in organisms. Some studies have also shown that PSTs can cause tissue damage and induce abnormal gene expression in *C. farreri*, but research on the changes of gene expression and regulatory mechanism of PST-induced tissue damage in *C. farreri* is still lacking. This information is important for establishing and perfecting food safety risk assessment technology.

In this study, *C. farreri* was exposed to a strain of *A. tamarense* (AT5-3). We measured the toxin

① Corresponding author: FENG Zhihua, E-mail: fengzhihua@jou.edu.cn; TAN Zhijun, E-mail: tanzj@ysfri.ac.cn

accumulation, oxidative stress kinase activity, and its transcriptional regulation in the visceral mass of *C. farreri* in control and experimental groups. Further, the ultrastructure of the visceral mass in the control group and the experimental group was observed to explore the initial stress response mechanism of *C. farreri* exposed to PSTs.

The 2-year-old scallop *C. farreri* was selected as the experimental animal. AT5-3 was cultured in L1 medium at temperatures of (20±1) ℃, light intensity of 54 μ/Em^2·s, and a light-dark ratio of 12 h:12 h in the laboratory, and *Chlorella vulgaris* was cultured simultaneously. The experimental group was fed with algal solution in the exponential growth period and the cell density was 4×10^4–4.2×10^4 cells/mL. The control group was fed with the same amount of *C. vulgaris*. The experiment lasted 20 days, of which the first six (days 0–6) were the exposure stage and the remaining 14 days (days 7–20) were the metabolic stage. During the exposure stage, *C. farreri* were fed regularly with the AT5-3 strain in exponential growth period twice a day with a feeding dose of 8×10^6 cells/items/day. The same amount of *C. vulgaris* was fed in the metabolic stage.

The results of toxin accumulation showed that paralytic shellfish toxins could accumulate rapidly in the visceral mass of *C. farreri*, but the metabolic rate was slow. The toxin content was highest on day 6 of the experiment, and the maximum accumulated content was approximately 15 times higher than the limit standard. The toxin residue reached its highest level (62.4%) on 20th day of the experiment.

The results of enzyme activity tests showed that the stress due to MDA, GSH-Px, and POD in the visceral mass was significantly increase (P<0.05), and the SOD activity was significantly inhibited (P<0.05) after a brief increase. The results also showed that PSTs could induce lipid peroxidation in *C. farreri*, and POD, SOD, and GSH-Px were significantly stressed to eliminate the adverse effects of PSTs.

The pathological changes in the visceral mass were observed under a transmission electron microscope and included vacuolation, chromatin aggregation, and nucleoplasmic pyknosis. Tissue damage worsened as the exposure time increased and although the toxin content in *C. farreri* decreased after the exposure period, the tissue damage was further aggravated. The results of transcriptome analysis showed that 933 differentially expressed genes (DEGs) were screened from the visceral mass of *C. farreri* after PST exposure. The results of KEGG and GO annotations showed that DEGs were mainly annotated in amino acid metabolism, energy metabolism, and other metabolic processes. Weighted gene co-expression network analysis showed that apoptosis and the glutathione metabolic detoxification pathway were significantly up-regulated, mapping *ALOX5*, *AfGST-σ11*, *caspase-8* and *Bax4* key transcription factors. In the experimental group, the expression of *ALOX5* and *AfGST-σ11* increased significantly when the accumulation rate was highest (P<0.05). The expression of *caspase-8* and *Bax4* was highest when toxin accumulation was high, which was significantly higher than that in the control group (P<0.05).

In summary, PSTs can cause lipid peroxidation stress and cell damage to *C. farreri*. In addition to antioxidant stress, *C. farreri* can activate characteristic apoptosis and resist PSTs toxicity by glutathione detoxification metabolism. However, this effect is limited and the persistent damage caused by high residual PSTs cannot be eliminated. This study provides a basis for further study on the potential toxicity of PSTs to the scallop *C. farreri* and its immunomolecular mechanisms.

Key words Paralytic shellfish toxin; *Chlamys farreri*; Physiological response; Apoptosis; Transcriptome